Available online at www.sciencedirect.com
ScienceDirect
Geomorphology 97 (2008) 483–501
GEOMORPHOLOGY
www.elsevier.com/locate/geomorph

Processes of coastal bluff erosion in weakly lithified sands, Pacifica, California, USA

Brian D. Collins [a,*], Nicholas Sitar [b]

[a] U.S. Geological Survey, Western Coastal and Marine Geology, 345 Middlefield Rd, MS-999, Menlo Park, CA 94025, United States
[b] Department of Civil and Environmental Engineering, University of California, Berkeley, 449 Davis Hall, Berkeley, CA 94720-1710, United States

Received 18 July 2007; received in revised form 1 September 2007; accepted 3 September 2007
Available online 14 September 2007

Abstract

Coastal bluff erosion and landsliding are currently the major geomorphic processes sculpting much of the marine terrace dominated coastline of northern California. In this study, we identify the spatial and temporal processes responsible for erosion and landsliding in an area of weakly lithified sand coastal bluffs located south of San Francisco, California. Using the results of a five year observational study consisting of site visits, terrestrial lidar scanning, and development of empirical failure indices, we identify the lithologic and process controls that determine the failure mechanism and mode for coastal bluff retreat in this region and present concise descriptions of each process.

Bluffs composed of weakly cemented sands (unconfined compressive strength — UCS between 5 and 30 kPa) fail principally due to oversteepening by wave action with maximum slope inclinations on the order of 65 at incipient failure. Periods of significant wave action were identified on the basis of an empirical wave run-up equation, predicting failure when wave run-up exceeds the seasonal average value and the bluff toe elevation. The empirical relationship was verified through recorded observations of failures. Bluffs composed of moderately cemented sands (UCS up to 400 kPa) fail due to precipitation-induced groundwater seepage, which leads to tensile strength reduction and fracture. An empirical rainfall threshold was also developed to predict failure on the basis of a 48-hour cumulative precipitation index but was found to be dependent on a time delay in groundwater seepage in some cases.
Published by Elsevier B.V.

Keywords: Coastal bluff; Sea cliff; Cemented sand; Weakly lithified sandstone; Failure mechanism; Wave climate; Landslide; Erosion

1. Introduction

The interaction between land and sea manifests itself most dramatically in the evolution of cliffs located at the coastal zone. In many parts of the world, bluffs composed of weakly lithified sediment undergo continuous erosion and in some cases, episodic landslide failure. The processes responsible for failure are often difficult to assess in these settings, due to the inaccessibility to document the events and the constantly changing morphology of the coast itself. For example, failures caused by direct wave action are typically not observable in-person and the post-failure morphology may undergo rapid change.

Despite these challenges and in response to societal need, researchers worldwide have sought to understand the processes contributing to coastal land loss. Existing case studies include those from England (Williams and Davies, 1987), France (Duperret et al., 2002), Italy (Budetta et al.,

* Corresponding author. Tel.: +1 650 329 5466; fax: +1 650 329 5190.
E-mail addresses: bcollins@usgs.gov (B.D. Collins), sitar@ce.berkeley.edu (N. Sitar).

0169-555X/$ - see front matter. Published by Elsevier B.V.
doi:10.1016/j.geomorph.2007.09.004

2000), Israel (Arkin and Michaeli, 1985) and Japan (Sunamura, 1982). In the United States, considerable effort has been made to document and assess bluff evolution, particularly on the west coast, including studies from Washington (Gerstal et al., 1998), Oregon (Komar and Shih, 1993), northern California (Griggs and Johnson, 1979; Hampton, 2002; Hapke and Richmond, 2002; Sallenger et al., 2002), and southern California (Kuhn and Osborne, 1987; Everts, 1991; Benumof and Griggs, 1999; Benumof et al., 2000). In many cases, the consequences of bluff failure have included the loss of homes and infrastructure, including most recently in northern California in 1998. This has been true along the bluffs located just south of San Francisco, California, in the city of Pacifica and which are the focus of this paper.

Investigations in the Pacifica area performed during the past 100 years include those following large storms (Bachus et al., 1981; Lajoie and Mathieson, 1998; Hampton and Dingler, 1998; Hampton, 2002; Snell et al., 2000; Sallenger et al., 2002) and earthquakes (Lawson, 1908; Bonilla, 1959; Plant and Griggs, 1990; Sitar, 1990). However, given this large body of work, a clear consensus has not been reached on the predominant failure mechanisms responsible for bluff retreat. For example, whereas Lajoie and Mathieson (1998) concluded that wave action is primarily responsible for bluff erosion, Hampton and Dingler (1998), in a study performed along several areas of northern California coastal bluffs including Pacifica, postulated that groundwater-induced seepage failures are sometimes more prevalent. They suggested that wave action may only play a secondary role by removing failed material from the base of the bluffs. Sallenger et al. (2002) suggested that there may be a balance between these two factors but were not able to reach a consensus from their data set.

This paper attempts to bring synergy to this debate and provide a framework for future coastal bluff erosion studies by identifying the failure mechanisms of a rapidly evolving but representative section of weakly lithified sand coastal bluffs. In this study, we provide descriptions of the observed failure modes and link these to the site-specific geology which varies throughout the study area. Observations of failures from five winter seasons (2001-2006), including several failures witnessed first-hand during storms, provide the bulk of data for generating our conclusions. High-resolution surface models, developed from terrestrial lidar laser scans performed periodically over this time, provide additional data for geomorphic analysis including crest retreat and failure geometry.

In our approach, we distinguish between failure mechanisms and failure modes. Coastal bluff failures are typically triggered by various forms of water-level change, wave action and toe erosion, terrestrial water (precipitation related surface or groundwater flow), weathering agents, freeze/thaw effects, and seismic shaking (see Hampton and Griggs, 2004); these are defined as failure mechanisms — the direct causes of the failures. Failure modes are defined as the method in which failures occur, whether by undercutting or oversteepening of the geometric profile of the bluff, by rotational failure, by tensile fracture caused by stress relief or loss of soil strength, or from lateral or vertical inertial forces from seismic shaking. Examples of research performed on specific types of failure modes include that on undercutting, notching, and toe oversteepening (Emery and Kuhn, 1982; Sunamura, 1982), rotational failure related to wave action and groundwater seepage (Quigley and Gélinas, 1976; Edil and Vallejo, 1980), stress relief fracturing and cantilevering (Hampton, 2002), and forces from seismic shaking (Sitar and Clough, 1983; Sitar, 1990; Ashford and Sitar, 2002). The modes are most often directly tied to the geometry of the bluff profiles, but can only be analyzed once the contributing mechanism has been identified.

2. Regional setting

The Pacifica coastal bluffs are located south of San Francisco, California along the Pacific coastline (Fig. 1). Our study area consists of seven bluffs (Fig. 2a), named according to their location either north or south of the site access point along a 1.5 km length of coast. The bluffs form the Mussel Rock marine terrace sequence as delineated by Smith (1960) and are composed of weakly lithified beach and dune sands interspersed with alluvial sediments.

Major bluff-forming units are estimated to be late Pleistocene and are capped with Holocene top soil, dune sand, and colluvium (Smith, 1960; Brabb and Pampeyan, 1983; Collins, 2004). Deposition occurred at or above beach level during a probable relative sea-level rise and during several periods of tectonically forced tilting (Smith, 1960). The terrace deposits overlie a complicated assemblage of lower Pleistocene paleosols and Mesozoic Franciscan Complex bedrock which form small headlands when exposed at beach level and commonly separate the coastline into distinct sections. The most prominent headland of the area is located immediately to the north of the Pacifica study area at Mussel Rock, where a splay of the San Andreas Fault crosses offshore to the northwest and which is partially responsible for the tilting of the deposits (Smith, 1960).

Provenance of the bluff deposits is determined by direct inspection of the cliff exposures. Paleo-dune deposits

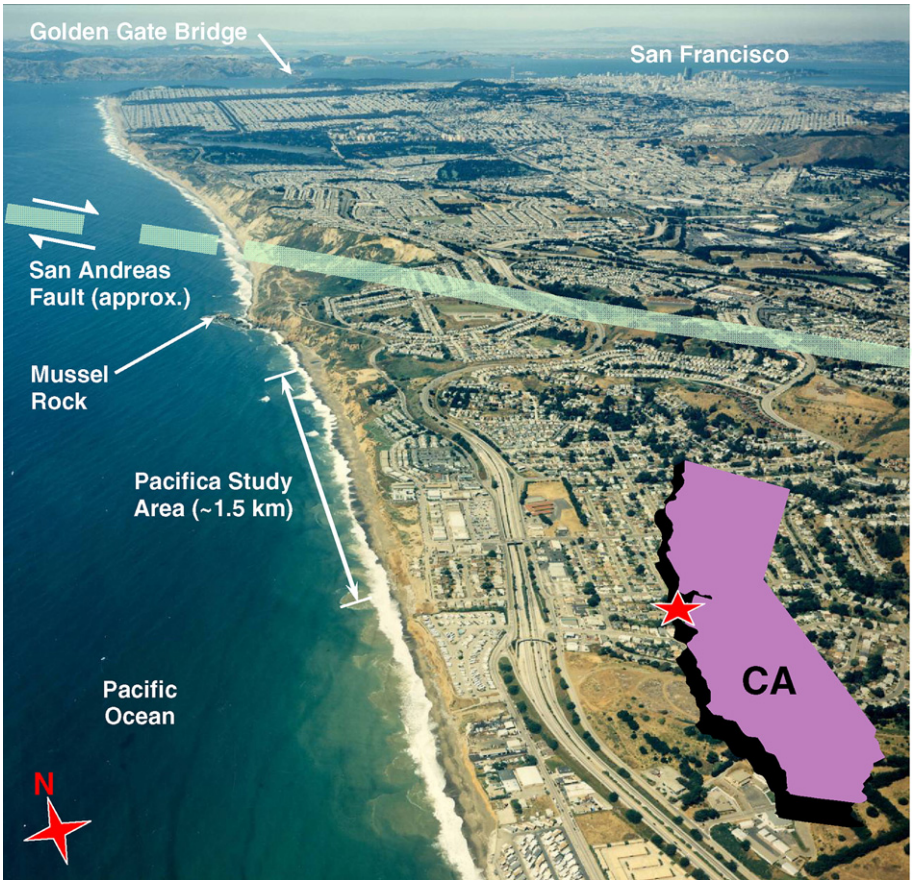

Fig. 1. Overview map of the Pacifica, California study area.

display broad sweeping cross-bed features over thicknesses of 10 m or more, whereas paleo-beach deposits are discerned by thin laminations with nonparallel planar bedding. Areas of alluvial deposition are less common and consist of pebbly channel sand and gravel where paleo-streams once drained seaward.

With respect to geotechnical characterization, the majority of units consist of very weakly to moderately cemented uniform sands according to categorical divisions proposed by Shafii-Rad and Clough (1982). The major bluff-forming sediments generally consist of two materials, herein referred to as "weakly cemented" and "moderately cemented" for simplicity. We differentiate the materials from one another qualitatively by a field test of slope inclination or quantitatively by their unconfined compressive strength (UCS). Bluffs that exhibit overall slopes with inclinations of more than 70° tend to be moderately cemented, whereas slopes that are 50–60° in inclination are weakly cemented. Geotechnical testing by Collins (2004) showed that the moderately cemented materials exhibit UCS up to 400 kPa and weakly cemented units are between 5 and 30 kPa. Thin section analysis by Bachus et al. (1981) on similar soils in the area showed that the moderately cemented sands are composed of more angular particles and contain more clay cementation bonds compared to the weakly cemented sands which are primarily bonded by iron oxide. Further, the void space has been measured to be between 6% and 13% less in these moderately cemented sands (Bachus et al., 1981; Collins, 2004). The lower degree of interlocking, particle contact points, and cementation are therefore responsible for the difference in strength in these materials.

Geologic mapping of portions of the study area has been performed by a number of researchers (Smith, 1960; Bachus et al., 1981; Brabb and Pampeyan, 1983; Howard-Donley Assoc., 1983; Lajoie and Mathieson, 1998; Sayre et al., 2001), however the mapping performed in the current study (Fig. 2b) is the first to identify the entire area in terms of geologic provenance and geotechnical characterization. Of particular note is the sharp distinction between weakly cemented sand units (Q_w and Q_{wu}) in the north–central portion of the bluffs and the moderately

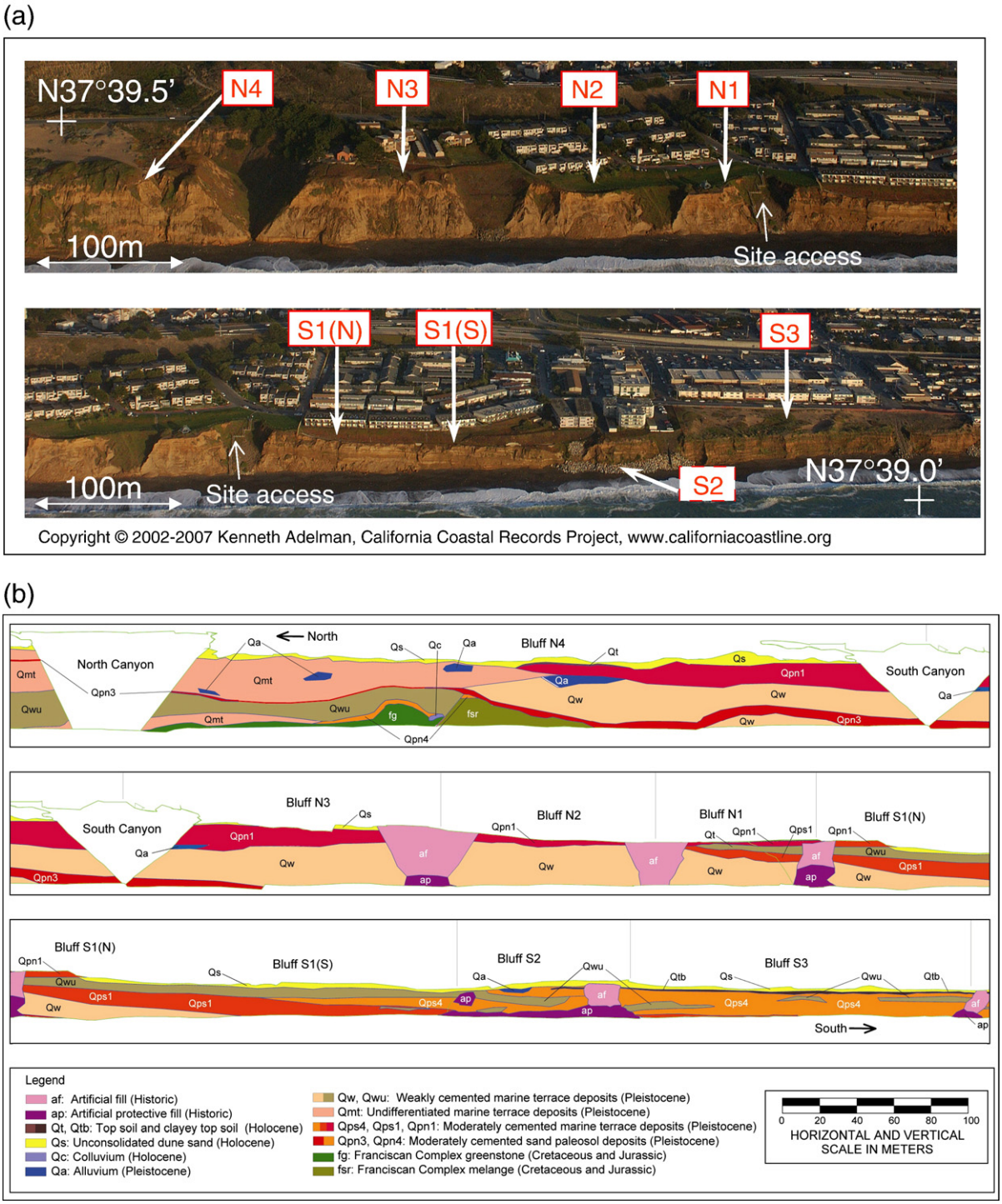

Fig. 2. (a) Profile panorama of study area. Bluff height ranges from 30 m in the north to 14 m in the south. Bluff S2 is stabilized with riprap and was not part of this investigation. (b) Geologic profile map of study area (after Collins, 2004). Individual Qw and Qp sub-units are grouped by their degree of cementation, and can be differentiated in the field as individual units.

cemented sand units ($Q_{p\_}$) located farther south. The intersection of the base of the Qps1 moderately cemented unit that forms the upper portions of Bluff S1(N) and the beach level marks this general division (Fig. 2a) Differential exposure to surface and ground water results in the various degrees of cementation. The spatial distribution of cementation is the primary factor responsible for the relative occurrence of different bluff failure mechanisms which is the focus of this paper.

3. Methods

3.1. Field observations

We made site-specific observations and compiled oblique photographs of the Pacifica coastal bluffs over a 5-year period to describe typical mechanisms and modes of bluff failure. Visits were made on a daily, weekly, or monthly basis over five winter seasons (November to May) between 2001 and 2006 and focused on seven individual bluffs (Fig. 2a). With the exception of Bluff S1(N) and S1(S), the bluffs are separated from one another by clearly defined, beach-perpendicular trending gullies. We divided Bluff S1 into two sections due to the change in material properties that occurs from north to south at beach level in this section (Fig. 2b). We did not observe Bluff S2 for native failures because this bluff is protected by slope grading and a 4.5 m-tall riprap revetment. In total, 128 visits were made over the five year period.

Visits consisted of walking the length of the beach at low tides and along the bluff crest to document changes in beach and bluff morphology. When a failure was observed, we determined the failure mechanism based on observations of the failure mode and the wave and weather conditions since the last field visit. Our observations documented the level of wave run-up on the beach and at the bluff toe based on strand lines and saturated bluff sediments, the presence or absence of seepage from the bluff face, typical failure dimensions, material type and maximum block size of failure debris, and the presence/absence of footprints or rainfall speckles on beach sand and debris following failure. These items provided evidence of failure timing, triggering mechanism, and associated crest retreat.

In all cases, determination of the associated failure mechanism was made using the best evidence presented by field observations and subsequent photographic interpretation. Although many winter storms resulted in both high levels of wave action and precipitation, we could typically determine the associated mechanism from the observations. For example, in failures of weakly cemented bluffs, the influence of precipitation could be judged as insignificant in many cases due to a lack of seepage in or near the crest or slope. On the other hand, the influence of wave action was directly obvious with large-magnitude changes occurring to the bluff toe and associated mid-bluff translational failures. The converse was also true — in the moderately cemented bluffs, precipitation had a very obvious effect in terms of seepage, and in the failure of blocks only located near the crest. High levels of wave action at the toe could not therefore be deemed responsible for these crest failures.

Whereas an attempt was made to document the occurrence of all magnitude of failures, we focused on identifying those failures that produced crest retreat. Thus, the presented data set represents only the largest magnitude events in the magnitude–frequency relationship for cliff failures in this area, and does not pinpoint smaller events that have also been shown to play a role in general coastal bluff evolution (e.g. Rosser et al., 2005). A majority of the photographic dataset is available for viewing at http://eriksson.gisc.berkeley.edu/bluff.

3.2. Empirical failure indices

Given our observations that wave action and precipitation contributed to failures on a regular basis, we developed proxies for their influence through representative indices of each failure mechanism. The maximum daily total water level (MD–TWL) on the beach during each failure period served as an index for the influence of wave action on bluff toe erosion. This index estimates the elevation of the water surface (relative to NAVD88) during maximum wave run-up taking into account waves, tides, storm surges and an indirect measure of beach slope (Collins, 2004; Collins et al., 2007). When the MD–TWL is greater than the bluff toe elevation, we can expect toe erosion and the instigation of wave-action driven failures. Conversely, when the MD–TWL is less than the bluff toe elevation, this is an indication that the bluff geometry should be stable. Detailed field visits performed during large storms in 2002–2003 clearly established this basis, with observations showing that waves reach the bluff toe intermittently for up to several (3+) consecutive hours during periods of high tide and wave activity.

Attempts to correlate actual toe elevations with MD–TWL have only been moderately successful however, due to constantly changing beach elevations that typify the active northern California coastline. We therefore compare MD–TWL with the winter seasonal average (November to May) of the MD–TWL to provide a relative measurement of “high” and “low” levels of wave action. Values of MD–TWL higher than the winter season

MD–TWL are therefore assumed to be more likely to cause toe erosion and subsequent bluff failure.

The MD–TWL was calculated from an empirical wave run-up equation (Ruggiero et al., 2001), developed for similar dissipative beaches along the Oregon coast. The Pacifica beach is also dissipative as measured by an Iribarren number (Battjes, 1974) ranging from 0.3 to 0.6 (Collins, 2004) and an average surf-scaling parameter (Guza and Inman, 1975) of 50 (Collins, 2004). In general, Iribarren numbers less than 1 are indicative of dissipative beaches (Aagaard and Masselink, 1999; Battjes, 1974), and surf-scaling parameters from 30 to over 100 categorize the dissipative extreme (Wright and Short, 1983). The wave run-up equation uses off-shore, deep water significant wave height data (H_s) (NOAA/NDBC, 2006) summed with local tide levels (η) (NOAA/NOS, 2006) to calculate the MD–TWL:

$$\text{MD–TWL} = \max(R_{2\%} + \eta) \quad (1)$$

where

$$R_{2\%} = 0.5H_s - 0.22(\text{Ruggiero et al., 2001}) \quad (2)$$

As a proxy for the influence of precipitation, we calculated the maximum 48-hour cumulative rainfall in the area during each failure period using available data from the National Weather Service (NWS, 2006). The 48-hour index, while empirical in nature, is justified analytically from a simple Darcy's Law evaluation of the vertical seepage velocity (V) through the bluff. Assuming a hydraulic conductivity (K) for uniform sand of 1×10^{-4} m/s (Craig, 1992) and an elevation driven hydraulic gradient ($i=1$), the seepage travel time (T) can be calculated for a position (D) in the lower mid-bluff area ($\sim$12 m below the crest):

$$T = D/V$$

where

$$V = Ki$$

such that

$$T = 12\text{m}/\left(1\times10^{-4}\text{m/s}\cdot1\right) = 33 \text{ hours}$$

We assume a conservative seepage travel time of 48 h to take into account run-off and longer travel time through less permeable materials during individual storms. Although the index does not evaluate actual seepage paths, groundwater flow, pore water pressures, or the obvious importance of multiple seepage faces within the bluff soils (Rulon and Freeze, 1985), we use it to evaluate relationships between storm precipitation, recorded failures and seasonal averages — storms with above season average precipitation totals should lead to failures more often.

3.3. Terrestrial lidar laser scanning

To obtain a geomorphic record of bluff and beach topography, we used a terrestrial lidar, laser scanning system (Fig. 3) on 17 occasions (Table 1). Our system consisted of a tripod-mounted Riegl Z210, 0.9 μm wavelength, Class 1 laser scanner with a 350-meter range and 15 mm point resolution (Riegl, 2007). The laser system uses a two-way, time of flight calculation of laser pulses measured along a precisely measured trajectory to build a "point cloud" of three-dimensional coordinates describing the geometry of the bluff, beach, and any other reflective object. The point cloud is post-processed to provide high-resolution (0.5 m maximum point to point spacing) surfaces and cross-sections for analysis including volumetric change, overall crest retreat, and failure morphology. Additional details of the data collection technique are described in Collins and Sitar (2004, 2005).

The laser scanner was mounted level on a tripod and data collected across a 180-degree swath centered on the bluffs. On each occasion, we collected 10 to 15 individual scans; each located about 100 m linearly apart along the beach. Scanning at periods of low tide from a distance of 50 m from the bluff resulted in an average point spacing of 10 cm on the bluff face. We used local reflectors to georeference the initial data set, and best-fit surface registration techniques to overlay consecutive scans from different dates. Processing of the point cloud data, including filtering, registration, georeferencing, and surface generation was performed using I-SiTE Studio software (I-SiTE, 2007). Surfaces were constructed using a spherical triangulation methodology designed to more accurately model steep and undercut topography such as that found in coastal bluffs. Volumetric changes and cross-sections were computed directly from the generated surfaces.

4. Results

4.1. Failure chronology

The results of the observation program are summarized in Tables 2 and 3 for the weakly and moderately cemented bluffs of the Pacifica study area. Here, we provide the date or range of dates when a failure occurred in a particular bluff, along with the identified failure mechanism from our observations. We also show the calculated empirical failure mechanism indices for both wave action and precipitation as described

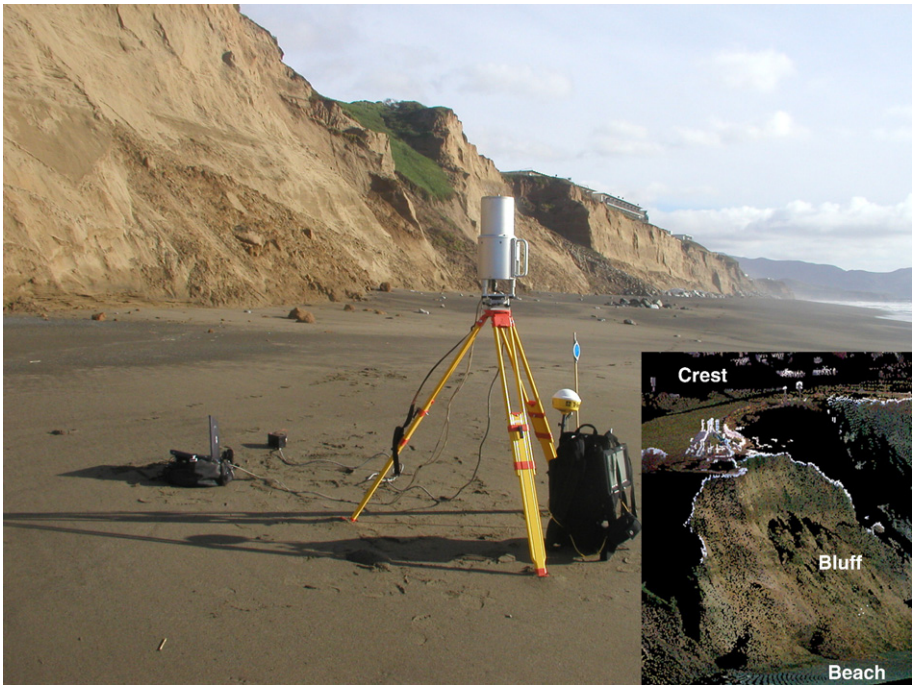

Fig. 3. Terrestrial lidar system for mapping three-dimensional coastal bluff topography. Laser is shown connected to laptop computer and battery. The general location of each scan is obtained using sub-meter DGPS, but data are registered using best-fit surface registration techniques. Blue reflector is typical of local reflectors positioned along the crest and used to georeference the data. Inset shows typical point data (~200,000 points) from registered scans located on the beach and the crest.

previously. In general, failures occurred from either wave action-induced changes to bluff slope geometry resulting in disaggregated debris slopes at the base of the bluffs (Fig. 4a) or from precipitation-induced groundwater and surface water seepage through the bluff profiles resulting in somewhat smaller debris volumes, but typically larger average debris block size (Fig. 4b). No significant crest retreat-inducing failures occurred

Table 1
Terrestrial lidar scanning chronology

Scan #	Date	Bluffs scanned[a]	Notes
1	10/14/2002	BN2, BN1, BS1	
2	01/14/2003	BN2, BN1, BS1	
3	03/03/2003	BN2, BN1, BS1	
4	05/08/2003	BN2, BN1, BS1	
5	11/06/2003	BN3, BN2, BN1, BS1, BS3	Lidar expanded to BN3 and BS3 in 2003
6	01/06/2004	BN3, BN2, BN1, BS1, BS3	
7	05/13/2004	BN3, BN2, BN1, BS1, BS3	
8	12/09/2004	BN3, BN2, BN1, BS1	
9	03/05/2005	Crest of BN2 and BN1 only	Data collection limited by dense fog
10	9/19+27/05	BN3, BN2, BN1, BS1, BS3	
11	12/12/2005	BN4, BN3, BN2, BN1, BS1, BS3	Lidar expanded to BN4 in 2005–06
12	01/05/2006	BN4, BN3, BN2, BN1, BS1, BS3	Crest topography also collected
13	02/08/2006	BN4, BN3, BN2, BN1, BS1, BS3	
14	03/08/2006	BN4, BN3, BN2, BN1, BS1, BS3	
15	04/06/2006	BN4, BN3, BN2, BN1, BS1, BS3	
16	04/25/2006	BN4, BN3, BN2, BN1, BS1, BS3	
17	06/06/2006	BN4, BN3, BN2, BN1, BS1, BS3	

[a] BS1 includes data for Bluff S1(N) and Bluff S1(S).

Table 2
Failure chronology of weakly cemented bluffs

	Failure date or range	Failure mechanism[a]	Approx. crest retreat[b] (m)	MD–TWL (m)	Max. 48-hour precip. (mm)	Lidar data of failure
Bluff N4[c]	11/1/2004–11/23/2004	Precipitation		3.35	19	
	1/7/2005–1/11/2005	Wave action	0.5	4.28	29	
	1/7/2005–1/11/2005	Wave action	0.3	4.28	29	
	4/19/2006–4/25/2006	Precipitation	2	2.78	1	Scan 16
Bluff N3	12/22/2001 – 12/29/2001	Wave action		3.90	31	
	12/30/2001–1/3/2002	Wave action		3.54	27	
	2/24/2004–2/25/2004	Wave action	0.5	4.43	37	
	3/11/2005–3/25/2005	Wave action	0.3	3.41	44	
	12/27/2005–1/3/2006	Wave action	0.5–1	4.62	80	
	12/27/2005–1/3/2006	Wave action		4.62	80	
	1/5/2006–1/8/2006	Wave action		3.38	4	
	2/3/2006–2/8/2006	Wave action	2–3	3.59	9	Scan 13
	4/6/2006–4/14/2006	Precipitation	0.5	3.80	21	Scan 16
Bluff N2	1/24/2002	Wave action	1 to 2	2.09	0	
	2/8/2002–3/19/2002	Wave action	2	3.60	37	
	12/13/2002 – 12/17/2002	Wave action	0.9	5.80	118	
	1/7/2003	Wave action	0.9	3.70	0	
	1/9/2003–1/10/2003	Wave action	0.2	2.70	24	
	1/12/2003–1/13/2003	Wave action	0.3	3.40	2	Scan 2
	1/22/2003	Wave action	0.9	2.70	5	
	1/28/2003–1/29/2003	Wave action	2.7	2.80	0	
	2/7/2003–2/11/2003	Wave action	0.6	2.30	0	
	2/13/2003–2/19/2003	Wave action	0.9	3.20	27	Scan 3
	3/15/2003–3/17/2003	Wave action	<0.1	3.80	42	
	12/4/2003 – 12/10/2003	Wave action	0.5	3.93	36	
	12/25/2003–1/6/2004	Precipitation	0.5	3.64	64	Scan 6
	2/27/2004–3/2/2004	Wave action	0.5–1.0	3.25	31	
	2/15/2005–2/25/2005	Precipitation	0.1	3.02	46	
	12/27/2005–1/3/2006	Wave action	1	4.62	80	Scan 12
	12/27/2005–1/3/2006	Wave action		4.62	80	Scan 12
	2/25/2006–3/4/2006	Wave action	2	4.15	55	Scan 14
	3/22/2006–3/28/2006	Precipitation		3.51	45	Scan 15
Bluff N1	1/7/2002–1/8/2002	Wave action		3.61	1	
	1/9/2002	Wave action	0.3	3.85	0	
	1/10/2002	Wave action	0.5	3.15	0	
	1/11/2002	Wave action	1	3.52	0	
	11/8/2002–11/9/2002	Wave action	<0.1	5.00	69	
	12/13/2002–12/17/2002	Wave action	2.4	5.80	118	
	12/19/2002	Wave action	1.2	5.10	48	
	1/12/2003–1/13/2003	Wave action	4.9	3.40	2	Scan 2
	1/22/2003	Wave action	0.9	2.70	5	
	1/28/2003–1/29/2003	Wave action	2.1	2.80	0	
	4/25/2003–5/3/2003	Wave action	1.4	2.90	41	Scan 4
	5/8/2003–5/16/2003	Wave action	0.3	3.80	1	
	11/5/2003–11/6/2003	Precipitation	0.5	2.09	7	Scan 5
	11/24/2003–12/10/2003	Wave action	0.5	3.93	36	
	12/25/2003–1/5/2004	Wave action		3.64	64	Scan 6
	3/16/2004–5/13/2004	Wave action		3.31	15	Scan 7
Bluff S1(N)	1/7/2002–1/8/2002	Wave action		3.61	1	
	1/9/2002	Wave action	0.3	3.85	0	
	1/10/2002	Wave action		3.15	0	
	12/13/2002–12/17/2002	Wave action	1.2	5.80	118	
	12/19/2002–12/20/2002	Wave action	0.9	5.10	56	
	12/26/2002–12/27/2002	Wave action	1.2	3.00	5	
	12/30/2002–1/6/2003	Wave action	1.2	4.50	14	Scan 2
	1/15/2003–1/22/2003	Wave action	2.4	3.00	5	
	1/31/2003–2/5/2003	Wave action	3.0	3.10	0	

Table 2 (*continued*)

	Failure date or range	Failure mechanism [a]	Approx. crest retreat [b] (m)	MD–TWL (m)	Max. 48-hour precip. (mm)	Lidar data of failure
Bluff S1(N)	4/25/2003–5/3/2003	Precipitation	<0.1	2.90	41	Scan 4
	12/22/2003–12/24/2003	Precipitation	0.2	4.13	19	
	12/25/2003–1/5/2004	Precipitation	0.3	3.64	64	Scan 6
	1/6/2004–1/17/2004	Precipitation		3.81	11	
	12/9/2004–1/4/2005	Precipitation	0.4	3.89	130	

[a] Identified failure mechanisms were determined by on-site observations and photo interpretation.
[b] Crest retreat is noted only where known; absence of a value indicates an unknown quantity.
[c] Observations of Bluff N4 began in 2004.

from either passive stress relief, seismic shaking, or other causes during the 5 winter seasons.

In the result tables, we also give an estimate of the associated crest retreat with each failure when known. Total crest retreat cannot be calculated from this data because failures did not occur in the same area of each bluff, nor over the full length of an entire bluff. However, total crest retreat at any point along the bluff edge can be calculated from the lidar data. When lidar data was collected in temporal proximity to a failure, it is noted in these tables.

4.2. Failure correlation with empirical indices

The empirical indices for the effects of wave action and precipitation on the weakly and moderately cemented bluffs provide an indication of the event magnitude that relates to expected failure. These results provide linkages between failure events and the identified failure mechanism and also establish baseline predictions for the event magnitude required to induce failure.

For wave action-induced failures of the weakly cemented bluffs, nearly all events occurred during periods of above average wave activity (Fig. 5, Table 2). While the average MD–TWL from the identified failures indicate a higher threshold (3.8 m), we feel that the best proxy for failure expectation is simply that of above average conditions as measured by the MD–TWL season average. Note that the majority of the weakly cemented bluff failures that were triggered by precipitation also occurred during above average wave action. As discussed, this is due to the combined effects of typical storms on the California coast, often bringing waves and rainfall concurrently.

For precipitation-induced failures in the moderately cemented bluffs, we find the 48-hour cumulative precipitation index to correlate well with a significant portion of the data. Most failures occurred during above-average precipitation totals (Fig. 6, Table 3). Here, we find a greater scatter of the results, but also find that the average 48-hour precipitation total for each failure (35 mm) is significantly above the season 48-hour storm average (15 mm). We note again, that whereas failures of these bluffs caused by the non-correlating mechanism (wave action in this case) occurred during high precipitation events, this is due to the concurrence of variable storm effects.

4.3. Failure morphology

The terrestrial lidar data sets provide unprecedented details of the failure morphology of the Pacifica bluffs. Cross-sections generated from the processed point clouds and surfaces (Figs. 7,8) show the configurations of the bluffs over time and over the spatial range of the study area during times when many failures were documented (Tables 2 and 3). Cross-sections for a single area of the weakly cemented bluffs (Fig. 8) show additional temporal detail of the bluff geometry, specifically with regard to the full cycle of failure, relative stability, wave erosion and additional failure. Periods of relative stability can be deduced from cross-sections that overlie one another, whereas periods of instability are indicated by steep cliff profiles followed by measurable crest retreat. Note that cross-sections often identify the geometry after failure; capturing the immediate pre-failure surface is rare, since changes to the toe often occur in the hours leading up to failure. Geomorphologic analyses of the overall bluff inclination (Fig. 8 — inset table) give direct evidence to the constantly evolving geometry of the bluffs. We use this type of analysis, along with that presented in Fig. 7, to formulate a clear description of the failure mechanisms and modes for these bluffs.

5. Analysis

Whereas the general processes of coastal bluff erosion are well known, these same general descriptions do not provide the necessary information to make detailed empirical or deterministic evaluations of bluff stability. Our results provide some of the best constrained observations of failures in both weakly and moderately cemented

Table 3
Failure chronology of moderately cemented bluffs

	Failure date or range	Failure mechanism [a]	Approx. crest retreat [b] (m)	MD–TWL (m)	Max. 48-hour precip. (mm)	Assoc. lidar data of failure
Bluff S1(S)	12/13/2002–12/16/2002	Wave action	0.6	5.8	118	
	12/17/2002	Precipitation	4.9 [c]	4.6	62	
	12/19/2002–12/20/2002	Precipitation		5.1	56	
	12/21/2002	Precipitation	0.9	4.1	22	
	12/27/2002–12/29/2002	Precipitation		4.2	50	
	12/30/2002–1/7/2003	Precipitation		4.5	14	Scan 2
	12/25/2003–1/6/2004	Precipitation	0.3	3.64	64	Scan 6
	3/16/2004–5/13/2004	Precipitation	0.1	3.31	15	Scan 7
	12/27/2005–1/3/2006	Wave action		4.62	80	Scan 12
	3/4/2006–3/8/2006	Wave action		3.80	39	Scan 14
	3/22/2006–3/28/2006	Precipitation	0.5–1	3.51	45	Scan 15
	4/6/2006–4/14/2006	Wave action		3.80	21	Scan 16
	5/1/2006–5/24/2006	Precipitation	2	3.22	6	Scan 17
Bluff S3	1/2/2002–1/3/2002	Precipitation		3.54	27	
	3/4/2003–3/12/2003	Precipitation		2.70	2	
	3/27/2003	Precipitation	0.9	2.90	2	
	4/12/2003–4/16/2003	Precipitation		3.20	48	
	4/24/2003	Precipitation	1.2	2.60	20	
	4/25/2003–5/5/2003	Precipitation		2.90	41	
	12/21/2003–1/6/2004	Precipitation	0.3	4.13	64	Scan 6
	1/6/2004–1/17/2004	Precipitation	0.1	3.81	11	
	3/16/2004–5/13/2004	Precipitation	0.05	3.31	15	Scan 7
	12/9/2004–1/4/2005	Precipitation	0.3	3.89	130	
	1/7/2005	Precipitation	0.1	4.28	14	
	4/14/2006–4/19/2006	Wave action	1–2	3.05	19	Scan 16

[a] Identified failure mechanisms were determined by on-site observations and photo interpretation.
[b] Crest retreat is noted only where known; absence of a value indicates an unknown quantity.
[c] Crest retreat for this event is anomalous and related to massive surface water gullying at the crest.

sands describing the timing and conditions required for cliff failure. Here, we utilize these results to provide detailed descriptions of the failure mechanisms and modes for each lithology as they pertain to weakly lithified sand coastal bluffs.

5.1. Coastal bluff erosion in weakly cemented bluffs from wave action-induced toe erosion

Our observations show a clear and definitive link between wave action-induced toe erosion and failures in

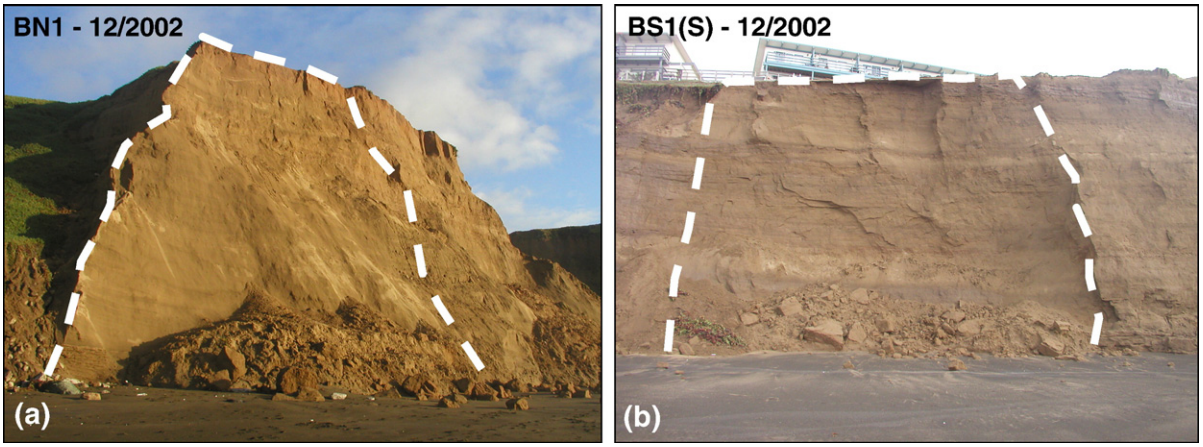

Fig. 4. Images showing areas of failure (dashed lines) in (a) weakly cemented materials from wave action, and (b) moderately cemented materials from precipitation-induced seepage. Note smoothed shear surface in (a) and rough, fractured surface in (b). Bluff height in (a) is 24 m. Bluff height in (b) is 18 m.

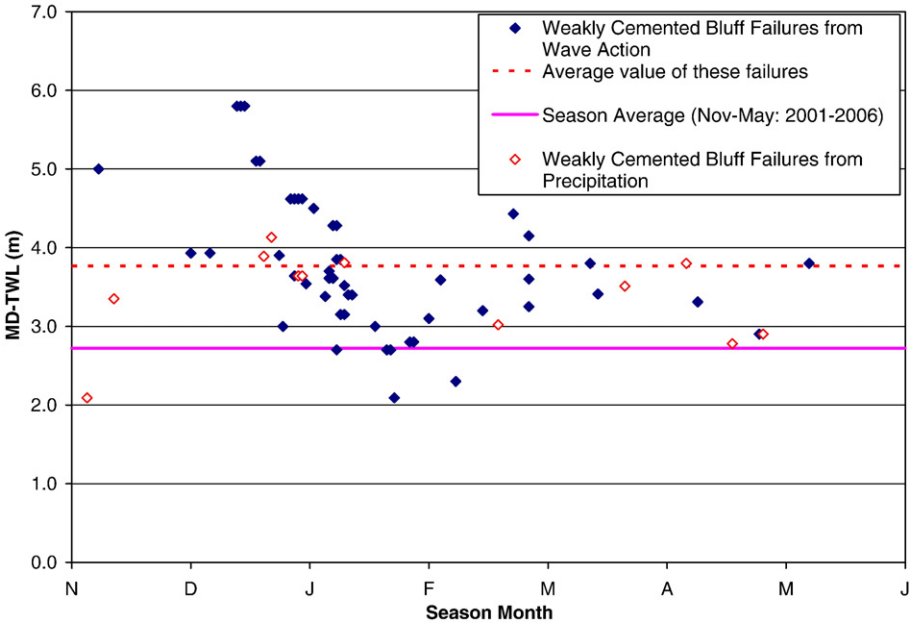

Fig. 5. Correlation of failures in weakly cemented bluffs with empirical index of wave action (MD–TWL) for the 2001–06 winter seasons. The average value of these failures (3.8 m) is 1.1 m above the season average. Values for failures caused by precipitation are shown for comparison.

weakly cemented coastal bluffs. Of the 62 failures recorded in these bluffs, 81% were related to wave action influences (Table 2). Specifically, we define wave action influences as those periods in which waves reached the bluff toe with sufficient energy to induce erosion of intact sediments.

Coastal bluff erosion begins with early winter-season beach lowering from wave-induced offshore transport of sand. For example, we measured a drop of 1.8 m between summer and winter beach height during the 2002–2003 season which allowed near-continuous wave contact during

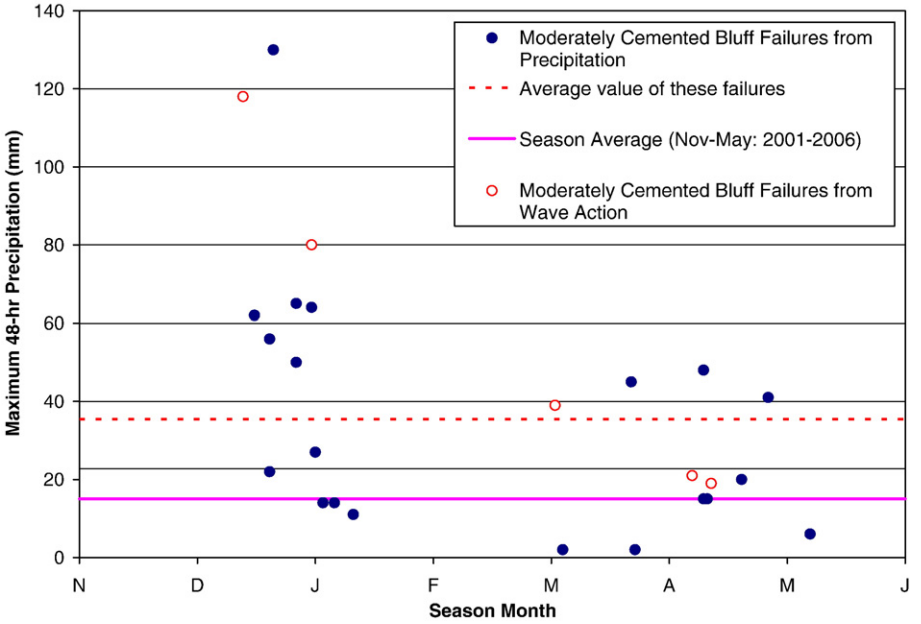

Fig. 6. Correlation of failures in moderately cemented bluffs with empirical index of precipitation (48-hour cumulative precipitation) for the 2001–06 winter seasons. The average value of these failures (35 mm) is 20 mm above the season average. The season average only includes those days with a non-zero value. Values for failures caused by wave action are shown for comparison.

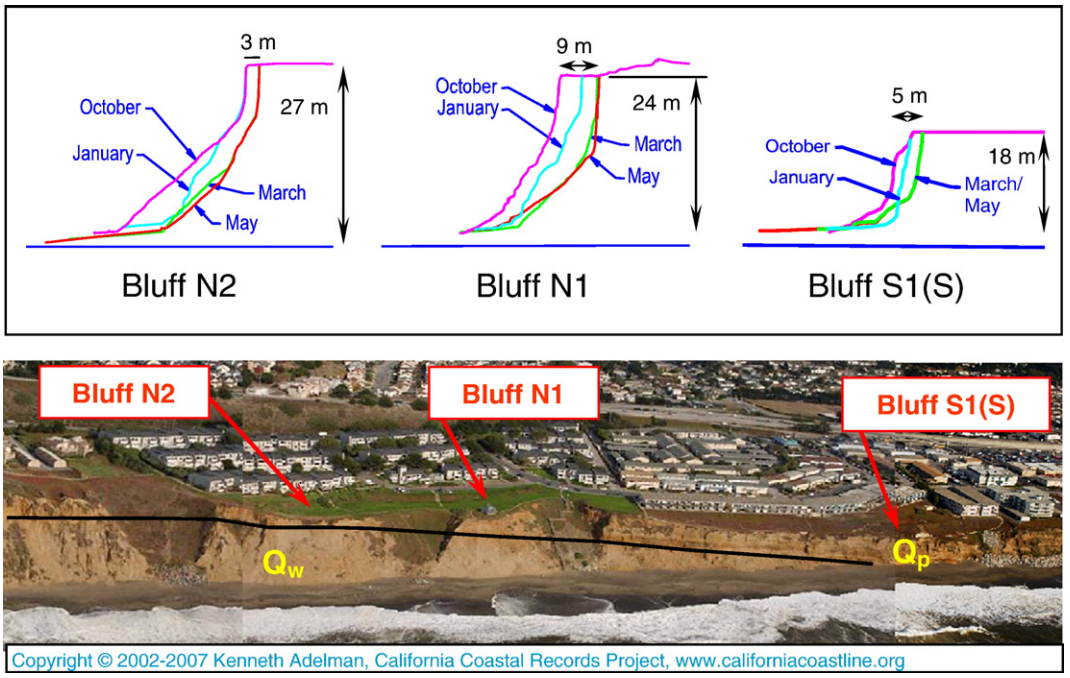

Fig. 7. Cross-sections from terrestrial lidar data from the 2002–03 winter season (October 2002, January, March, May 2003) and corresponding images of three bluffs showing the transition from a wave action driven failure mode in weakly cemented lithology (Q_w — Bluffs N2 and N1), to a precipitation-induced seepage driven failure mode in moderately cemented lithology (Q_p — Bluff S1(S)). Geologic units are consistent with Fig. 2.

periods of winter high tide. Higher wave energy associated with winter-season, north-Pacific storms also leads to an increase in direct wave action at the bluff toe. Based on offshore buoy climatology data collected by NOAA/NDBC (2006), the defined winter (November through April) significant wave height (2.1 m) is 0.6 m above the

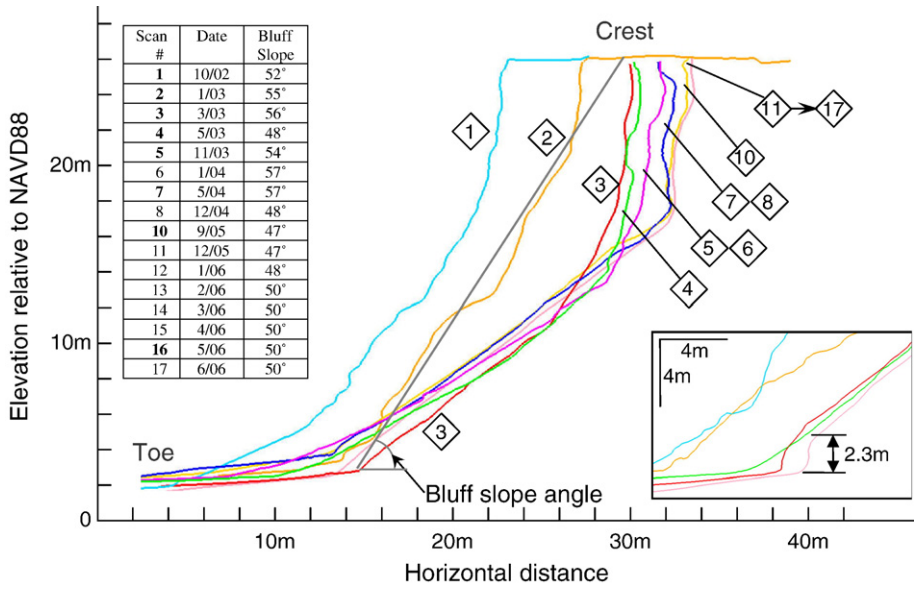

Fig. 8. Cross-sections from terrestrial lidar data of Bluff N1 beginning in 2002 through 2006. Diamond labels indicate order of scans (inset table and Table 1, only Scans #'s in bold are shown for simplicity). The bluff slope angle is measured from the intersection of the beach and bluff toe to the bluff crest. No scan was collected during September 2005 (Scan #9). Minor sloughing of the crest occurred between May 2004 and September 2005 that was not associated with a major failure event. Inset shows cross-section located 20 m to the south that more clearly identifies vertical toe geometry required for failure.

summer (May through October) average. Similarly, the average winter wave period (8.2 s) is also greater than the summertime average by 1.4 s. In these winter conditions, waves break approximately 200 m offshore, reforming two or three times as a less coherent swash front on their way up the near-shore and beach front. When beach, tide, and wave conditions allow, we have seen wave swash make contact with the bluff toe for several hours during a single high-tide cycle. Lidar-derived elevation data of the beach and bluff (Fig. 8) indicates that the beach-toe intersection regularly reaches elevations of only 2 to 3 m and the failure observations show that a majority of failures occur when the total water level on the beach reach or exceed these elevations (Table 2, Fig. 5).

The wave swash erodes toe material by a reverse seepage mechanism, similar to rapid drawdown conditions along river banks (e.g. Springer et al., 1985; Dapporto et al., 2003). In a coastal setting, the near-vertical slope toe is saturated by incoming water and fails seaward as the returning water drains from the soil, whether composed of previously failed debris or intact material. Tension cracks forming behind the new slope may fill with sea water as the next wave reaches the toe, causing additional instability. Undercutting of the toe from wave action in the intact, weakly cemented material does not occur in the strictest sense — the bluff forming materials are sufficiently weak such that the near-vertical toe fails as an inclined wedge prior to any undercut (i.e. cantilevered section) forming. Retrogressive bluff failure occurs as steeper profiles form, but with nearly identically inclined shear planes (Fig. 9). Our observations (Fig. 10), along with the lidar data (Fig. 8), indicate that the maximum vertical height of the toe scarp reaches 2 to 3 m during each stage of failure evolution. The toe scarp height

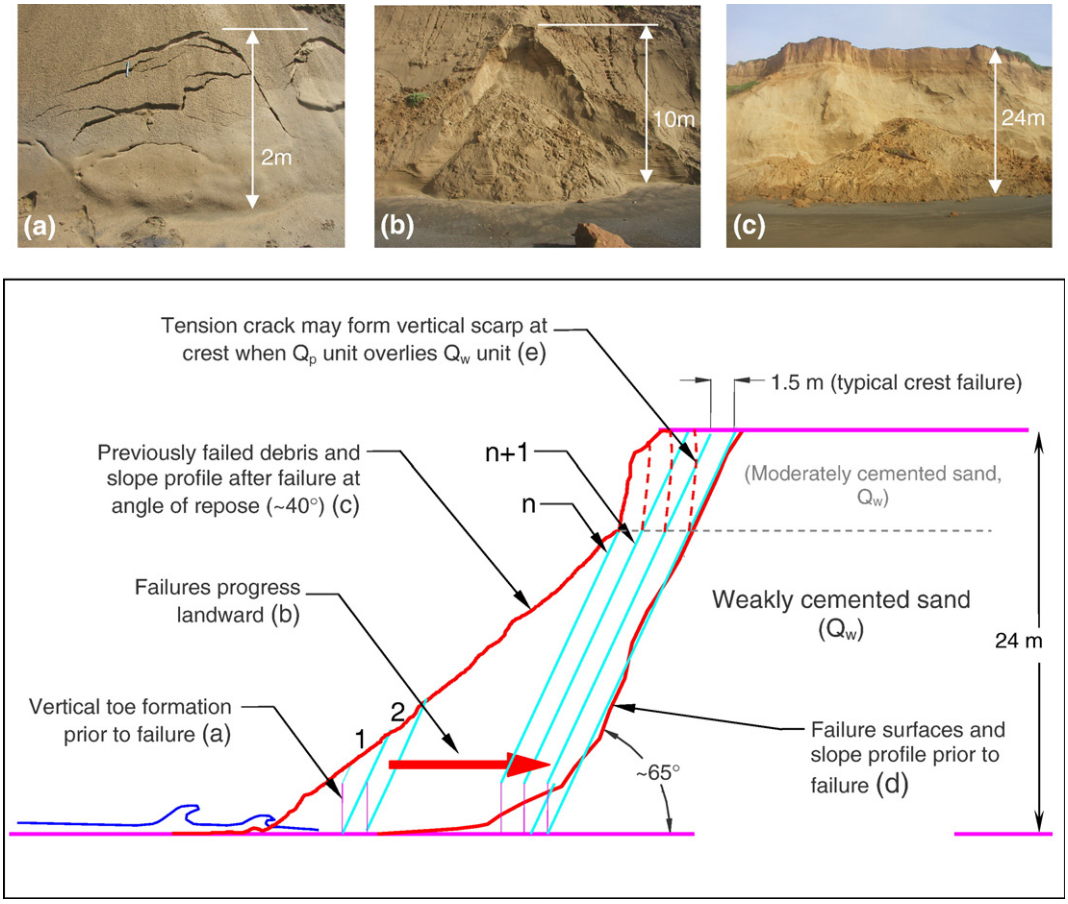

Fig. 9. Geomorphic model of wave action-induced bluff failure with typical profiles from lidar data shown. Waves acting only on previously failed debris results in small, slab failures less than 2 m high (a). Shear failures increase in height (1, 2, *n*) (b), but without crest retreat, as waves erode into either previously failed debris or into unfailed, intact material (c). Failure along the entire bluff height occurs at $n+1$ with resultant crest retreat along parallel shear planes (d). The cycle will start anew as the resulting debris is eroded by wave action. At Pacifica, moderately cemented sand (Q_p) overlies the weakly cemented sand at the crest and forms vertical scarps (e) that fail in response to wave action induced toe erosion occurring beneath (see also Figs. 7 and 8).

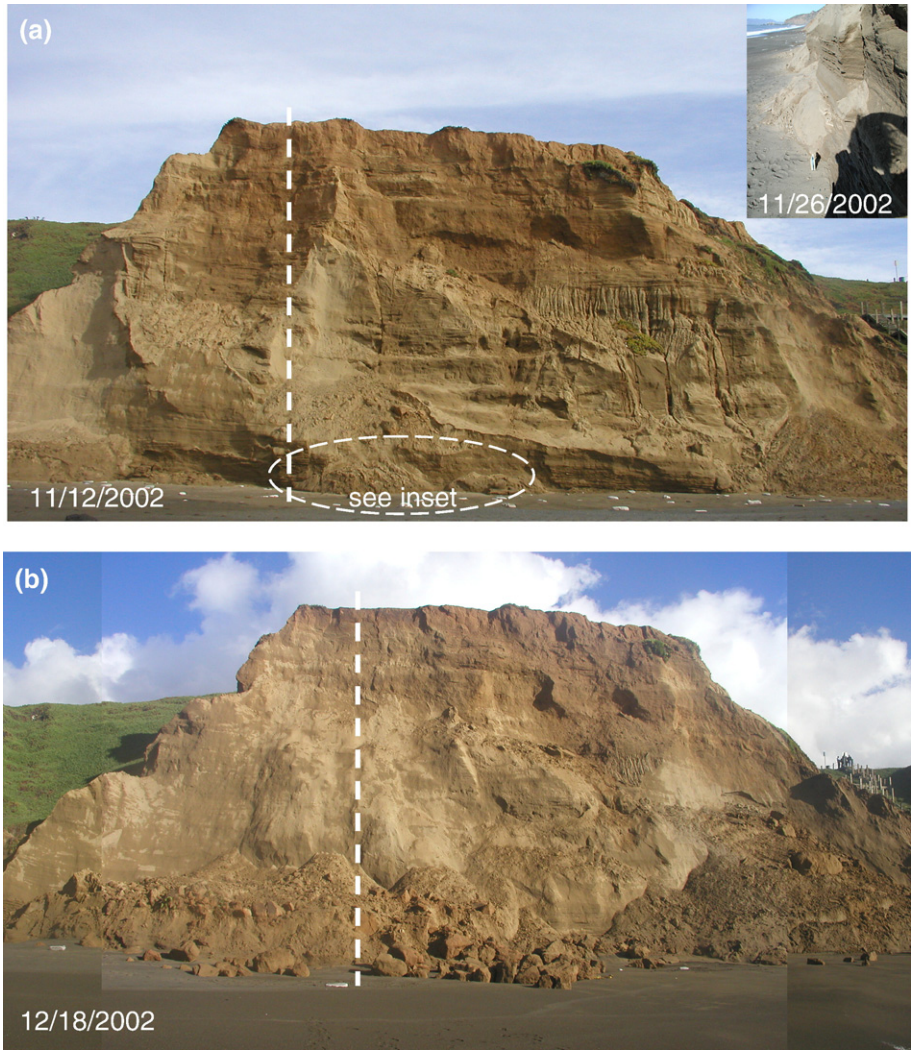

Fig. 10. Weakly cemented bluff geometry of Bluff N1 before (a) and after failure (b). Failure occurred in mid-December, 2002 (Table 2: 12/13–17/2002) along nearly the whole length of bluff — the unfailed central area failed several weeks later. Bluff height is 24 m. Dashed straight lines indicate location of cross-sections in Fig. 8. Inset in (a) shows absence of undercutting in 2-meter tall vertical toe through intact, horizontally bedded lithology, several weeks before failure.

is limited by the geotechnical strength characteristics of the soil; geotechnical testing (Collins, 2004) has shown that the cohesive strength of the weakly cemented sand is only 6 kPa and not capable of forming taller, vertical configurations. Whereas the overall slope inclination typically varies between 45 and 60° (Fig. 8), lower and mid-slope inclinations can reach up to 65°, with upper slope areas reaching near-vertical in the moderately cemented sand layer capping these bluffs (Figs. 8, 9). The combination of a vertical toe scarp profile and a steep (~65°) mid-slope inclination is typically the configuration that precedes failure (Figs. 9, 10).

Typical crest retreat resulting from complete bluff failure is about 1.0 m, although 4.9 m has been recorded from a single event (Table 2 – Bluff N1). Intact blocks up to 1.5 m in greatest dimension are often found on the beach following these failures. The crest blocks, along with the bulk of the failure debris, provide a temporary defense against immediate continued failure through a combination of toe buttressing and erosion protection, but in effect are themselves the beginning of the next failure cycle (Figs. 8, 9). Winter seasons without observed failures (e.g. 2002–03 at Bluff N3 and 2004–06 at Bluff N1, Table 2) are indicative of these periods with large deposits of previously failed material located at the toe (Fig. 8, Scans 7–17). Smaller failures at the crest that do not lead to entire bluff failure will continue to occur during this time from terrestrial processes, and may result in

minor, yet measurable, crest retreat that should be anticipated.

5.2. Coastal bluff erosion in moderately cemented bluffs from precipitation-induced seepage

Failures resulting from wave action do not occur in the moderately cemented bluffs as often due to their higher resistance against cyclical wave impact. The higher resistance has been measured in geotechnical laboratory tests (Collins, 2004) which show that unconfined compressive strength is more than 25 times higher in the moderately cemented materials (340 kPa) compared with the weakly cemented materials (13 kPa). This also explains why these bluffs form much taller near-vertical slope sections, commonly extending the entire height of the bluff (Fig. 4b). During this study, 20 failures in the moderately cemented bluffs (80%) were directly attributable to precipitation-induced failure mechanisms (Table 3, Fig. 6). Additional precipitation-induced failures also occurred along the geologic transition area in the southern portion of Bluff S1(N), further validating this failure mechanism in bluffs composed predominantly of moderately cemented material.

The results (Table 3) indicate that the average 48-hour rainfall required for bluff failure was 35 mm (Fig. 6). This magnitude is typical for winter storms of the northern California coast; the maximum 48-hour event exceeded 68 mm for each winter of this study (Collins et al., 2007). For those cases with minimal recorded precipitation (less than the season average — Fig. 6), the full data set of daily precipitation values (Collins et al., 2007) indicates that a significant storm event preceded each of these failures by several days to a week. We interpret at least some of these anomalies to be related to particularly long seepage pathways that trigger failure only upon reaching specific, and potentially lower elevation, tensile stress compromised areas of the bluff.

The failure process (Fig. 11) begins with precipitation from passing storms collecting in the subsurface behind the crest of the bluffs, moving downward into the moderately cemented materials, and ponding on distinct, less

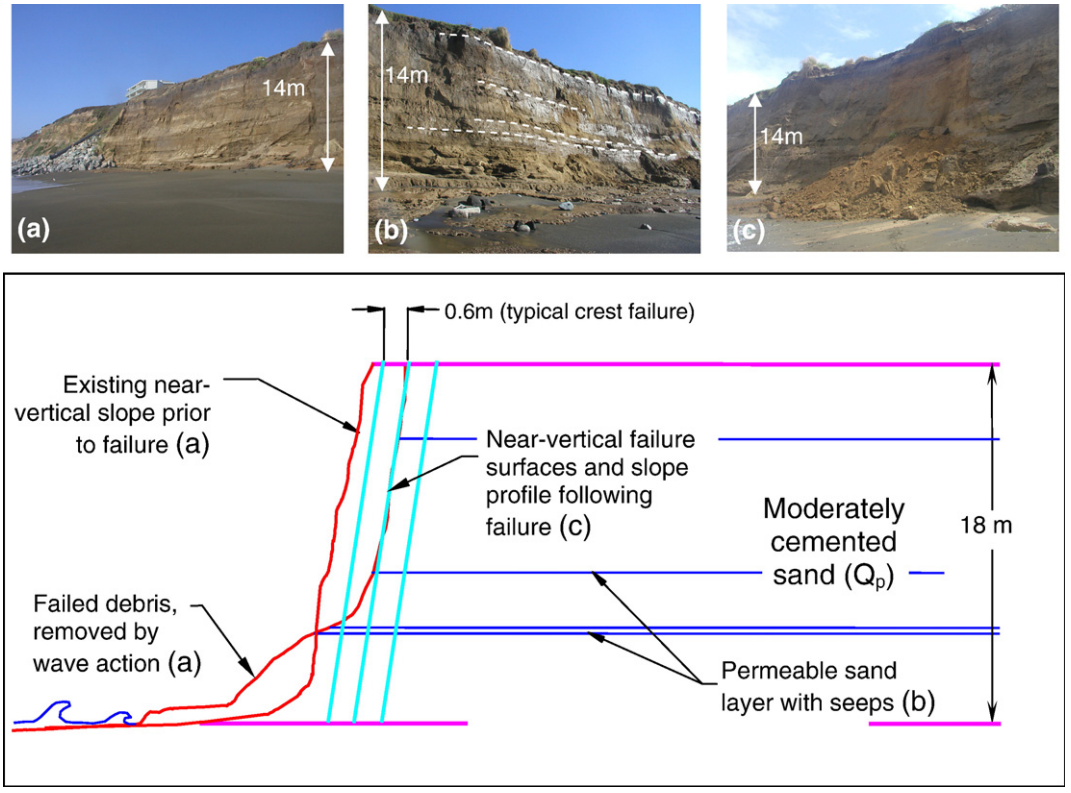

Fig. 11. Geomorphic model of precipitation-induced seepage bluff failure with typical profiles from lidar data shown. The bluff geometry is near-vertical with previously failed debris removed by wave action (a). Water moves downward through the soil profile, ponding on denser layers (b), and visible as seeps in the bluff face. Loss of tensile strength lead to slab failures located above the dense, ponding layers (c). Failed debris may buttress the bluff profile until removed by wave action, however a vertical geometric profile is already established in the upper portions, ready for additional failures.

permeable layers of material. Water flows along these boundaries, exiting at the bluff face, or passes through the layer, eventually perching on the next less permeable layer beneath it. Similar observations have been made in coastal cliffs in California (Norris and Back, 1990), Oregon (Komar, 2004) and the Great Lakes region (Sterrett and Edil, 1982). Multiple opportunities for ponding may exist with a heterogeneous distribution of pore pressures throughout the bluff profile, consistent with analyses by Rulon et al. (1985).

Site-specific geotechnical testing performed in conjunction with this study (Collins, 2004) has shown that the tensile strength of these materials is reduced from −32 kPa when dry to −6 kPa when wet. Hampton (2002) also showed an indirect decrease in the tensile strength upon wetting through site-specific measurements of soil cohesion and correlations by Sitar et al. (1980). Given typical tensile stress levels between -5 and -10 kPa (Sitar and Clough, 1983, Collins, 2004), ponded water reduces the tensile strength of the materials beyond the tensile stress levels of the bluff geometry. This dislodges slabs of less dense material located immediately above the ponding surface, consistent with the stress–relief fracturing mode identified by Hampton (2002) in these bluffs. While positive pore water pressures could develop and lead to a similar process, the tensile stress–strength analysis shows that this point is not necessary for failure.

Our observations indicate that failures in these bluffs occur only from a failure in tension and fracture; signs of shear failure, such as slickensides along the remaining bluff face were not observed. Typical failures are on the order of 0.1 to 1.2 m deep (measured into the bluff) with associated average crest retreat of 0.6 m (Table 3). Due to the higher cohesion of the moderately cemented material, debris from failures may reside at the base of the cliffs for lengthier periods of time before being completely removed by wave action, compared with weakly cemented failure debris. Thus, while we maintain that precipitation is the primary failure mechanism for these bluffs, we also acknowledge that wave action is the mechanism responsible for sustaining the vertical profile at the base of the bluffs, a process identified as the "passive-effect" of wave-action (e.g. Edil and Vallejo, 1980). This, in turn, allows a tensile fracture failure mode to potentially occur with the next passing storm.

Of note is that seepage seems to have only a minimal effect on the stability of the weakly cemented bluffs. Our observations indicate that these soils readily allow seepage without ponding, thus minimizing the residence time of water within the sediments. Failures in the thin capping layer of moderately cemented sand that overlies the weakly cemented sands in the northern bluffs (Fig. 2) do occur occasionally, but do not contribute to failure of the entire height of the bluff.

6. Discussion

Our observations and analyses show that there are two predominant failure mechanisms in the Pacifica area, and that their role is dependent on the material strength of the bluffs. Given the varying lithology over the several kilometers of bluffs in this region, it is not surprising that previous researchers have reached different conclusions over the predominant failure mechanisms and modes. For example, Bachus et al. (1981) observed many deep-seated type failures toward the north end of the Pacifica area. While not the major focus of this study, our geologic mapping of these areas found predominantly weak greenstone of the Franciscan Complex overlain by weakly cemented sands – typical conditions for deeper-seated sliding based on the stronger nature of the underlying but weathered bedrock. Lajoie and Mathieson's (1998) observations of the Pacifica region made during the 1982–82 El Niño winter, showed areas of active block falls and debris slides but did not report any large-scale failures from wave action, especially in the northern portion of our study area. Sitar (1983) on the other hand, did identify wave erosion as one of the failure mechanisms in this area several years earlier. Our observations have shown clear evidence for the strong effects of wave action in the same areas observed by these previous researchers. However, we do not find these observations in contradiction, rather, we conclude and verify the premise that failures in weakly cemented bluffs do not occur repeatedly during every storm season. Wave action must remove previously failed debris before the bluff is susceptible to the next round of failures (Figs. 8 and 9). Finally, we address Hampton and Dingler's (1998) and Hampton's (2002) work, who found that stress relief-induced exfoliation and groundwater seepage were the primary mechanisms in large portions of the Pacifica area. Again, we find our observations and analyses in agreement with their conclusions; however we also find that these mechanisms are only predominant in the moderately cemented lithologic units found in the southern portion of the study area and continuing southward along the coast from this point.

Of particular note is that none of these preceding studies identified wave-cut notching as a significant factor in coastal bluff retreat in this region. Despite the often-thought assumption that this is the typical failure mode, we also found no strong evidence for this and argue that this point is not minor — it is of importance

when considering the timing, magnitude and particularly in the geotechnical analysis of failures.

We therefore offer the following suggestions for practitioners working in coastal bluff topography:

- The horizontal and vertical extents of exposed lithology and the associated geologic units unconfined compressive strengths and tensile strengths can be used to effectively determine which failure mechanism and mode may be more prevalent.
- In weakly cemented bluffs, it is recommended to use the maximum slope inclination, as measured between the toe and crest or within the mid-slope area, as a proxy for relative bluff stability rather than solely on the absence or presence of toe undercutting.
- Following wave action-induced failures, terrestrial processes such as groundwater and surface water flow, and stress release-induced exfoliation, will continue to evolve the upper portions of the bluff, as wave action erodes the failed debris at the toe. This crest retreat should be anticipated.
- In moderately cemented bluffs, failures will be triggered by high precipitation events in the absence of wave action. However, wave action is the ultimate driving force to achieve the steep topography required for the generation of tensile stresses in the bluff face and subsequent precipitation-induced seepage failures.

In summary, our research shows the importance of careful geologic mapping of both horizontal and vertical distributions of sediment and/or rock types. This study also highlights the benefits of long-term monitoring and observation, which has also been noted by other coastal researchers (Rosser et al., 2005). Each lithologic unit can be linked to a specific failure mode — it is the proper identification of the spatial and temporal variability in the processes that provides additional insight. We therefore recommend that similar methodologies be used for coastal bluff investigations in other areas, particularly within similarly exposed, similar age, marine terrace deposits along the west coast of the United States.

7. Conclusions

This study identified the spatial and temporal processes responsible for erosion and landsliding in an area of weakly lithified sand coastal bluffs located in northern California, USA. Our observations and analyses, made over five consecutive winter seasons and consisting of detailed site visits and high resolution terrestrial lidar scans, provide new insight into the failure mechanics of these coastal bluffs. Specifically, we identified the lithologic and process controls that determine the failure mechanism and mode for coastal bluff retreat in this region and presented concise descriptions of each process. Our descriptions highlight the key observations that must be accounted for when performing geomorphologic and geotechnical stability assessments of these and other similar coastal bluffs. Weakly cemented sand bluffs fail due to wave action-driven erosional changes in the slope profiles with maximum slope inclinations of up to 65° prior to failure. Moderately cemented sand bluffs fail due to precipitation-induced groundwater seepage that leads to tensile strength reduction and tensile fracture. Subsequent wave action maintains the steep bluff profiles over time, allowing additional seepage-related failures. Empirical correlations developed in this study provide an estimate for predicting the conditions in which future failures may occur. For wave action-induced failure in weakly cemented bluffs, above season-average values of the MD–TWL index (2.7 m) show a clear correlation with observed failures and their average MD–TWL average (3.8 m). In the moderately cemented bluffs, a 48-hour cumulative precipitation index was utilized as a correlation index with failures. A similar relationship was extracted, with the average 48-hour precipitation value for these failures (35 mm) significantly exceeding the seasonal storm average (15 mm). The observed mechanisms of failure, while not new to coastal bluff research, had not been fully quantified in this area of the northern California coast. These observations, coupled with the newly developed empirical relationships, should provide additional assistance to the prediction and evaluation of coastal bluff stability in the future.

Acknowledgments

Funding for this research was provided by grants from the U.S. Geological Survey, Western Region Coastal and Marine Geology Program, the University of California, Coastal Environmental Quality Initiative (CEQI), and the U.S. Geological Survey, Mendenhall Postdoctoral Program. The authors wish to thank Monty Hampton for valuable insights of the study area and for technical review of the manuscript and Robert Kayen for collaboration with the USGS terrestrial lidar system. Bijan Khazai, Pamela Patrick, and Ann Marie Puzio, former graduate students at University of California-Berkeley, and Diane Minasian and Gregory Gabel of the USGS assisted with the data collection and processing efforts. Scott Schiele from I-SiTE Laser Imaging was

instrumental in assisting with the lidar processing and initial data collection. Technical reviews of this manuscript by Cheryl Hapke (USGS), Gerald Weber, and two other anonymous reviewers are gratefully appreciated. The photo in Fig. 1 is used with permission from Cotton, Shires and Associates and the photos in Figs. 2 and 7 are used with permission of the California Coastal Records Project. Their cooperation is gratefully acknowledged.

References

Aagaard, T., Masselink, G., 1999. In: Short, A.D. (Ed.), The Surf Zone, Handbook of Beach and Shoreface Morphodynamics. Wiley, Chichester, England, pp. 74–82.

Arkin, Y., Michaeli, L., 1985. Short- and long-term erosional processes affecting the stability of the Mediterranean coastal cliffs of Israel. Engineering Geology 21, 153–174.

Ashford, S.A., Sitar, N., 2002. Simplified method for evaluating seismic stability of steep slopes. Journal of Geotechnical Engineering 128 (2), 119–128.

Bachus, R.C., Clough, G.W., Sitar, N., Shafii-Rad, N., Crosby, J., Kaboli, P., 1981. Behavior of weakly cemented soil slopes under static and seismic loading conditions, Volume II. The John A. Blume Earthquake Engineering Center, Report No. 52. Stanford University, Stanford, California. July 1981, 247pp.

Battjes, J.A., 1974. Surf Similarity, Proceedings 14th Int. Conf. on Coastal Engineering. Copenhagen, Denmark, pp. 466–480.

Benumof, B.T., Griggs, G.B., 1999. The dependence of seacliff erosion rates on cliff material properties and physical processes: San Diego County, California. Shore and Beach 67 (4), 29–41.

Benumof, B.T., Storlazzi, C.D., Seymour, R.J., Griggs, G.B., 2000. The relationship between incident wave energy and seacliff erosion rates: San Diego County, California. Journal of Coastal Research Vol. 16 (4), 1162–1178.

Bonilla, M.G., 1959. Geologic observation in the epicenter area of the San Francisco earthquake of March 22, 1957. In: Oakshot, G.B. (Ed.), California Division of Mines Special Report 57. California Division of Mines, Sacramento, CA, pp. 25–37.

Brabb, E.E., Pampeyan, E.H., 1983. Geologic map of San Mateo County, California, U.S. Geological Survey Miscellaneous Field Studies Map I-1257-A, Scale 1:62,500, U.S. Geological Survey, Menlo Park, California.

Budetta, P., Galietta, G., Santo, A., 2000. A methodology for the study of the relation between coastal cliff erosion and the mechanical strength of soils and rock masses. Engineering Geology 56 (3–4), 243–256.

Collins, B.D., 2004. Failure Mechanics of Weakly Lithified Sand Coastal Bluff Deposits: Doctoral dissertation. University of California, Berkeley. 278pp.

Collins, B.D., Sitar, N., 2004. Application of high resolution 3D laser scanning to slope stability studies. Proceedings of the 39th Symposium on Engineering Geology and Geotechnical Engineering, Butte, Montana, May 18-21, 2004, pp. 79–92.

Collins, B.D., Sitar, N., 2005. Monitoring of coastal bluff stability using high resolution 3D laser scanning. In: Rathje, E.M. (Ed.), ASCE Geo-Frontiers Special Publication 138:- Site Characterization and Modeling, Remote Sensing in Geotechnical Engineering. ASCE, Austin, Texas. Jan 24-26, CD-ROM.

Collins, B.D., Kayen, R., Sitar, N., 2007. Process-based empirical prediction of landslides in weakly lithified coastal cliffs, San Francisco, California, USA. In: McInnes, R., Jakeways, J., Fairbank, H., Mathie, E. (Eds.), Landslides and Climate Change: Proc. of the Int. Conf. on Landslides and Climate, Isle of Wight, UK. Taylor & Francis, pp. 175–184.

Craig, R.F., 1992. Soil Mechanics, 5th Edition. Chapman and Hall, London. 423 pp.

Dapporto, S., Rinaldi, M., Casagli, N., Vannocci, P., 2003. Mechanisms of riverbank failure along the Arno River, central Italy, Earth Surf. Process. Landforms 28, 1303–1323.

Duperret, A., Genter, A., Mortimore, R.N., Delacourt, B., De Pomerai, M.R., 2002. Coastal rock cliff erosion by collapse at Puys, France, the role of impervious marl seams within chalk of NW Europe. Journal of Coastal Research 18 (1), 52–61.

Edil, T.B., Vallejo, L.E., 1980. Mechanics of coastal landslides and the influence of slope parameters. Engineering Geology 16, 83–96.

Emery, K.O., Kuhn, G.G., 1982. Sea Cliffs: their processes, profiles, and classification. Geological Society of America Bulletin 93, 644–654.

Everts, C.H., 1991. Seacliff retreat and coarse sediment yields in southern California. Quantitative Approaches to Coastal Sediment Processes, Seattle, Washington, pp. 1586–1598.

Gerstal, W.J., Brunengo, M.J., Lingley, W.S., Logan, R.L., Shipman, H., Walsh, T.J., 1998. Puget Sound Bluffs: the where, why, and when of landslides following the holiday 1996/97 storms. Washington Geology 6 (1), 17–31.

Griggs, G.B., Johnson, R.E., 1979. Coastline erosion, Santa Cruz County. California Geology April, 67–76.

Guza, R.T., Inman, D.L., 1975. Edge waves and beach cusps. Journal of Geophysical Research 80 (21), 2997–3012.

Hampton, M.A., 2002. Gravitational failure of sea cliffs in weakly lithified sediment. Environmental and Engineering Geoscience 8 (3), 175–192.

Hampton, M.A., Dingler, J., 1998. Short term evolution of three coastal cliffs in San Mateo County. California, Shore and Beach 66 (4), 24–30.

Hampton, M.A., Griggs, G.B., 2004. Formation, evolution, and stability of coastal cliffs: status and trends, U.S. Geological Survey Professional Paper 1693. 123pp. (http://pubs.er.usgs.gov/usgspubs/pp/pp1693).

Hapke, C., Richmond, B., 2002. The impact of climatic and seismic events on the short-term evolution of seacliffs based on 3-D mapping: northern Monterey Bay. California, Marine Geology 187, 259–278.

Howard-Donley-Associates, 1983. Geotechnical investigation — seacliff stability analysis. Shoreline Protection Assessment District, Esplanade-Palmetto Avenue, Pacifica, California, Consulting report.

I-SiTE Inc., 2007. "3D Laser Scanning Software", 1 April 2007. http://www.isite3d.com.

Komar, P.D., Shih, S.-M., 1993. Cliff erosion along the Oregon coast: a tectonic-sea level imprint plus local controls by beach processes. Journal of Coastal Research 9 (3), 747–765.

Kuhn, G.G., Osborne, R.H., 1987. Sea cliff erosion in San Diego County, California. Advances in Understanding of Coastal Sediment Processes, New Orleans, Louisiana, pp. 1839–1918.

Lajoie, K.R., Mathieson, S.A., 1998. 1982-83 El Niño Coastal Erosion, San Mateo County. U.S. Geologic Survey Open-File Report 98-041, CA. 61pp.

Lawson, A.C., 1908. California earthquake of April 18, 1906: publication no 87. Report to the State Earthquake Investigation Committee, Vol. 1. Carnegie Institute of Washington, Washington, D.C.

National Oceanic and Atmospheric Association. National Data Buoy Center, (NOAA/NDBC) Site #46026, San Francisco, California. (online), http://seaboard.ndbc.noaa.gov/.

National Oceanic and Atmospheric Association. National Ocean Service, (NOAA/NOS) Observed Water Levels and Associated Ancillary Data (online), Site #9415020, Point Reyes, California. http://co-ops.nos.noaa.gov/data_res.html.

National Weather Service (NWS) Forecast Office. San Francisco Bay Area/Monterey (online), Site # Pacifica 2S, Pacifica, California (PCAC1). http://www.wrh.noaa.gov/Monterey/rtp02/.

Norris, R.M., Back, W., 1990. Erosion of seacliffs by groundwater. In: Higgins, C.G., Coates, D.R. (Eds.), Groundwater Geomorphology; the role of subsurface water in Earth-surface processes and landforms. Geological Society of America, Boulder, Colorado, pp. 283–290.

Plant, N., Griggs, G.B., 1990. Coastal landslides caused by the October 17, 1989 Earthquake, Santa Cruz County. California: California Geology 43 (1), 75–84.

Quigley, R.M., Gélinas, P.J., 1976. Soil mechanics aspects of shoreline erosion. Geoscience Canada 3 (3), 169–173.

Riegl, 2007. "Terrestrial Scanning Laser Systems", 1 April. 2007 <http://www.rieglusa.com>.

Rosser, N.J., Petley, D.N., Lim, M., Dunning, S.A., Allison, R.J., 2005. Terrestrial laser scanning for monitoring the process of hard rock coastal cliff erosion. Quarterly Journal of Engineering Geology and Hydrogeology 38, 363–375.

Ruggiero, P., Komar, P.D., McDougal, W.G., Marra, J.J., Beach, R.A., 2001. Wave runup, extreme water levels and the erosion of properties backing beaches. Journal of Coastal Research 17 (2), 407–419.

Rulon, J.J., Freeze, R.A., 1985. Multiple seepage faces on layered slopes and their implications for slope stability analysis. Canadian Geotechnical Journal 22, 347–356.

Rulon, J.J., Rodway, R., Freeze, R.A., 1985. The development of multiple seepage faces on layered slopes. Water Resources Research 21 (11), 1625–1636.

Sallenger, A.H., Krabill, W., Brock, J., Swift, R., Manizade, S., Stockdon, H., 2002. Sea-cliff erosion as a function of beach changes and extreme wave runup during the 1997–1998 El Niño. Marine Geology 187, 279–297.

Sayre, T., Shires, P.O., Skelly, D.W., 2001. Mitigation of 1998 El Nino Sea Cliff Failure, Pacifica, California. In: Ferriz, H., Anderson, R. (Eds.), Engineering Geology Practice in Northern California. CDMG/AEG, pp. 607–618.

Shafii-Rad, N., Clough, G.W., 1982. The Influence of Cementation on the Static and Dynamic Behavior of Sands: The John A. Blume Earthquake Engineering Center, Report No. 59. Stanford University, Stanford, California. December 1982, 315pp.

Sitar, N., 1983. Slope stability in coarse sediments. In: Yong, R. (Ed.), Special Publication on Geological Environment and Soil Properties. ASCE, pp. 82–98.

Sitar, N., 1990. Seismic response of steep slopes in weakly cemented sands and gravels. Proc. of H. B. Seed Memorial Symp., Berkeley, California, May 19, 1990, Vol. 2. Bitech Publishers, Vancouver, B. C., pp. 67–82.

Sitar, N., Clough, G.W., 1983. Seismic response of steep slopes in cemented soils. Journal of Geotechnical Engineering 109 (2), 210–227.

Sitar, N., Clough, G.W., Bachus, R.C., 1980. Behavior of weakly cemented soil slopes under static and seismic loading conditions. Report No. 44, The John A. Blume Earthquake Engineering Center. Stanford University, Stanford, California.

Smith, D.D., 1960. The geomorphology of part of the San Francisco Peninsula. California, Ph.D. Dissertation. Stanford University, Menlo Park, California. 356pp.

Snell, C.B., Lajoie, K.R., Medley, E.W., 2000. Sea-cliff erosion at Pacifica, California caused by the 1997/98 El Niño storms,: Slope Stability 2000. ASCE Geot. Spec. Pub. No. 101, Proc. of Geo-Denver, Denver, Colorado, pp. 294–308. August 5-8, 2000.

Springer Jr., F.M., Ullrich, C.R., Hagerty, D.J., 1985. Streambank stability. Journal of Geotechnical Engineering 111 (5), 624–640.

Sterrett, R.J., Edil, T.B., 1982. Ground-water flow systems and stability of a slope. Ground Water 20 (1), 5–11.

Sunamura, T., 1982. A predictive model for wave-induced cliff erosion, with application to Pacific coasts of Japan. Journal of Geology 90, 167–178.

Williams, A.T., Davies, P., 1987. Rates and mechanisms of coastal cliff erosion in lower Lias rocks. Advances in Understanding of Coastal Sediment Processes, New Orleans, Louisiana, pp. 1855–1870.

Wright, L.D., Short, A.D., 1983. Morphodynamics of beaches and surf zones in Australia. In: Komar, P.D. (Ed.), Handbook of Coastal Processes and Erosion. CRC Press, Boca Raton, Florida, pp. 43–53.